

## RESEARCH ARTICLE

10.1002/2014JA020541

## Key Points:

- Modeling premidnight plasma density troughs observed in Alaska in summer
- Density troughs occur during weak solar and magnetic activity
- Model indicates cause is convection of low-density plasma from lower latitudes

## Correspondence to:

P. G. Richards,  
prichar1@gmu.edu

## Citation:

Richards, P. G., M. J. Nicolls, J.-P. St.-Maurice, L. Goodwin, and J. M. Ruohoniemi (2014), Investigation of sudden electron density depletions observed in the dusk sector by the Poker Flat, Alaska incoherent scatter radar in summer, *J. Geophys. Res. Space Physics*, 119, 10,608–10,620, doi:10.1002/2014JA020541.

Received 26 AUG 2014

Accepted 3 DEC 2014

Accepted article online 5 DEC 2014

Published online 20 DEC 2014

## Investigation of sudden electron density depletions observed in the dusk sector by the Poker Flat, Alaska incoherent scatter radar in summer

P. G. Richards<sup>1</sup>, M. J. Nicolls<sup>2</sup>, J.-P. St.-Maurice<sup>3</sup>, L. Goodwin<sup>3</sup>, and J. M. Ruohoniemi<sup>4</sup>

<sup>1</sup>School of Physics, Astronomy and Computational Sciences, George Mason University, Fairfax, Virginia, USA, <sup>2</sup>Center for Geospace Studies, SRI International, Menlo Park, California, USA, <sup>3</sup>Institute of Space and Atmospheric Studies, Saskatoon, Saskatchewan, Canada, <sup>4</sup>Virginia Tech, Bradley Department of Electrical and Computer Engineering, Blacksburg, Virginia, USA

**Abstract** This paper investigates unusually deep and sudden electron density depletions (troughs) observed in the Poker Flat (Alaska) Incoherent Scatter Radar data in middle summer of 2007 and 2008. The troughs were observed in the premidnight sector during periods of weak magnetic and solar activity. The density recovered to normal levels around midnight. At the time when the electron density was undergoing its steep decrease, there was usually a surge of the order of 100 to 400 K in the ion temperature that lasted less than 1 h. The Ti surges were usually related to similar surges in the AE index, indicating that the high-latitude convection pattern was expanding and intensifying at the time of the steep electron density drop. The convection patterns from the Super Dual Auroral Radar Network also indicate that the density troughs were associated with the expansion of the convection pattern to Poker Flat. The sudden decreases in the electron density are difficult to explain in summer because the high-latitude region remains sunlit for most of the day. This paper suggests that the summer density troughs result from lower latitude plasma that had initially been corotating in darkness for several hours post sunset and brought back toward the sunlit side as the convection pattern expanded. The magnetic declination of  $\sim 22^\circ$  east at 300 km at Poker Flat greatly facilitates the contrast between the plasma convecting from lower latitudes and the plasma that follows the high-latitude convection pattern.

### 1. Introduction

The interaction between the solar wind, magnetosphere, and ionosphere takes place even during very quiet conditions. It is well known that under very quiet conditions the convection pattern shrinks to higher latitudes while the *Kp* and global magnetic storm indices like the *Dst* (the 1 h resolution Disturbed Storm) and *Sym-H* (the 1 min resolution symmetric *H* component of the magnetic field around the earth) remain very low during quiet conditions. There are nonetheless several oscillations in the course of a day in the *AE* or *AL* and *AU* indices on a scale of the order of 100 to 300 nT and lasting between 1 and 3 h per event. These indices are associated with the auroral electrojet currents. A maximum in the *AE* is therefore associated with intensification in the auroral electrojet current and can be associated with the occurrence of substorms which are considered to be small if the *AE* stays below 300 nT. These small substorms are often not accompanied by major ring current injection events in the sense that the *Sym-H* or *Dst* indices indicate a complete absence of magnetic storm.

The latest solar minimum was particularly weak with the consequence that the solar wind produced few intense magnetic storms. This has provided an opportunity to study the system under particularly weakly driven conditions. One noticeable point is that weak substorms continued to be present, as evidenced by typical oscillations of the order of 300 nT or less in the *AE* occurring several times per day. The International Polar Year (IPY) has been timely for the study of these weakly driven conditions with a large array of ground-based ionospheric monitoring instruments providing an unusually high-density of temporal coverage. One such instrument was the Poker Flat Incoherent Scatter Radar (PFISR) located in near Fairbanks, Alaska. The radar was routinely pointed along the geomagnetic field direction from which it could examine the electron density and the ion and electron temperatures. From time-to-time, convection electric field data were retrieved by pointing some of the radar beams to the north of its location.

Measurements by the Poker Flat Incoherent Scatter Radar (PFISR) in summer 2007–2008 revealed deep electron density depletions (troughs) associated with strong westward convection velocities in the premidnight sector. The electron density could decrease by an order of magnitude and be much smaller than at midnight when the solar zenith angle (SZA) was actually larger. Such large and sudden density depletions cannot be explained by normal nighttime decay because the SZA remains below  $93^\circ$  at Poker Flat. The investigation is limited to summer because the identification of premidnight density depletions is not possible at other seasons when the sun sets early and the density decreases to very low values after sunset.

The density depletions were often accompanied by abrupt ion temperature (Ti) increases of  $100\text{--}400^\circ$  above the ambient temperature of  $\sim 750^\circ$  for  $\sim 1\text{--}2$  h in the premidnight hours. *Goodwin et al.* [2014] discuss properties of the Ti spikes and ascribe their cause to a temporary increase in the ion-neutral frictional heating near the high-latitude convection boundary. The detection of this phenomenon has been facilitated by the continuous running of PFISR and also because of the special conditions provided by the weak magnetic activity in the solar minimum of 2007–2008.

*Goodwin et al.* [2014] proposed that either the electric field was systematically stronger when the overall convection pattern was intensifying or that the privileged location of spikes was related to the presence of neutral winds that had a strong antisunward component, prior to encountering the newly sunward convecting ions. The strong electric field strengths would be consistent with Sub-Auroral Polarization Streams (SAPS) although SAPS occurrence has not been related to weak substorms and summer conditions [*Foster and Burke*, 2002].

This paper is primarily focused on the sudden electron density depletions that are normally associated with the Ti Spikes. The radar encounters the sudden drops in density premidnight and then the density rises sharply to a normal nighttime level even though the SZA is still near its maximum value. The phenomenon is observed to occur at times of strong magnetically westward convection. It is proposed that the sudden density depletions are caused by convection to Poker Flat of lower latitude plasma, which has been corotating and decaying for several hours after sunset prior to being caught in the expanding convection pattern and being brought to the sunlight regions.

## 2. Measurements

The Poker Flat Incoherent Scatter Radar (PFISR) is located at the Poker Flat Research Range near Fairbanks, Alaska ( $65^\circ\text{N}$ ,  $213^\circ\text{E}$ ). PFISR is the first incoherent scatter radar (ISR) that uses phased array technology to steer on a pulse-to-pulse basis over a limited field-of-view [*Heinselman and Nicolls*, 2008]. Furthermore, the modern design of the system allows it to be operated remotely and continuously.

The operating mode for the International Polar Year (IPY) and normal background monitoring consists of low-duty cycle ( $\sim 1\%$ ) transmissions and one to four look directions, including one beam directed up the local magnetic field line (data from which are used in this study). Transmissions for the IPY mode consist of a  $480\ \mu\text{s}$  ( $72\ \text{km}$ ) long pulse for  $F$  region studies interleaved with a  $4.5\ \text{km}$  resolution alternating code for  $E$  region studies. Data are typically processed at 15 min integration periods because of the low-duty cycle, although higher time resolutions (up to  $\sim 5$  min) are available during high SNR conditions. The normal analysis consists of fits for the electron density, electron temperature, ion temperature, and line-of-sight component of the ion velocity. Electron densities are calibrated using daytime measurements of the plasma line. For more details on the IPY operations [see *Sojka et al.*, 2009].

Second-order products such as  $h_m F_2$  and  $N_m F_2$  were derived from the data when densities were sufficiently high and when the layer profile was suitable for the determination of those parameters (e.g., during times of particle precipitation, this was not usually possible). The  $h_m F_2$  and  $N_m F_2$  values were found by applying polynomial fits to the electron density profiles near the peak of the layer.

The derivation of neutral winds from the PFISR data was previously described by *Richards et al.* [2009]. Winds along the magnetic meridian were derived from  $F$  region field-aligned motions using techniques standard for midlatitude observatories [e.g., *Salah and Holt*, 1974; *Buonsanto and Witasse*, 1999; *Aponte et al.*, 2005]. This approach corrects the field-aligned ion motion for ambipolar diffusion effects using the NRLMSISE-00 background neutral atmosphere model and interprets the remaining component of the motion as due to the projection of the magnetically southward wind. The large magnetic dip angle at PFISR ( $\sim 77.5^\circ$ ) makes the

technique error prone. For example, a 100 m/s neutral wind will result in line-of-sight velocities in the range of 10–20 m/s. In addition, enhanced diffusion due to ion upflow driven by auroral processes, will bias the wind estimates.

### 3. Model

The field line interhemispheric plasma (FLIP) model has been developed over a period of more than 30 years as a tool specifically designed to improve our understanding of the physics and chemistry of the ionosphere [Richards *et al.*, 1998, 2000, 2009, 2010; Richards, 2001, 2002, 2004]. It incorporates the basic chemical scheme that was developed from the AE mission but is continually updated as more information becomes available.

The FLIP model is a one-dimensional (1-D) model that calculates the plasma densities and temperatures along entire magnetic flux tubes from below 100 km in the Northern Hemisphere through the plasmasphere to below 100 km in the Southern Hemisphere. The flux tubes can also move under the influence of electric fields.

The continuity and momentum equations for  $O^+$ ,  $H^+$ ,  $He^+$ , and  $N^+$  and the energy equations for ion and electron temperatures are solved with a flux-preserving formulation together with a Newton iterative procedure [Torr *et al.*, 1990]. Secondary ion production and thermal electron heating due to photoelectrons is provided by a solution of the two-stream photoelectron flux equations using the method of Nagy and Banks [1970]. The photoelectron solutions have been extended to encompass the entire field line on the same spatial grid as the ion continuity and momentum equations. Chemical equilibrium densities are obtained for  $NO^+$ ,  $O_2^+$ ,  $N_2^+$ ,  $O^+(^2P)$ , and  $O^+(^2D)$  ions below 500 km altitude in each hemisphere. The densities of minor neutral species  $NO$ ,  $O(^1D)$ ,  $N(^2D)$ , and  $N(^4S)$  are obtained by solving continuity and momentum equations in each hemisphere. The model also solves for the first five excited states of vibrationally excited  $N_2$ , which is important because the  $O^+$  loss rate is enhanced by vibrational excitation.

The present model calculations were performed using the NRLMSISE-00 model neutral density [Picone *et al.*, 2002] and solar EUV irradiances measured by the Solar EUV Experiment (SEE) instrument on the TIMED satellite [Woods *et al.*, 2008]. The model solar EUV irradiances are daily average TIMED-SEE irradiance measurements for the summer of 2007 and 2008 that were obtained from the Laboratory for Atmospheric and Space Physics Interactive Solar Irradiance Data Center on 1 August 2012.

Accurate modeling of the ionospheric electron density requires a faithful reproduction of the variations in height of the  $F_2$  layer ( $h_mF_2$ ) because that determines the altitude distribution of the electron density and its peak density. At subauroral latitudes, the altitude variations of  $h_mF_2$  are primarily determined by the component of the neutral winds in the magnetic meridian direction. However, at all latitudes there is also a contribution from zonal electric fields, which is typically smaller during the weak magnetic activity periods. Both the wind and zonal electric field components are captured by using the algorithm of Richards [1991], which adjusts the model wind to accurately follow the measured  $h_mF_2$ . The resultant winds, which are in the magnetic meridian, are termed equivalent or effective winds due to the possible zonal electric field component. At midlatitudes the electric field component is usually small and the equivalent winds have been found to agree well with optical and radar inferred winds including those from PFISR [Dyson *et al.*, 1997; Richards *et al.*, 2009]. The inferred neutral winds in the magnetic meridian are available from an analysis of the radar field-aligned ion velocities, and these generally agree well with the equivalent winds deduced from  $h_mF_2$ . Optically measured neutral winds are not available in summer at Poker Flat because the solar zenith angle is too small. In any case, ionosphere models need the electric field component as well as the neutral wind component along the magnetic meridian.

### 4. Results

This section shows samples of PFISR data and model results for weak magnetic activity periods during the summer of 2007 and 2008. During these time periods, the solar activity was low with the 81 day average  $F_{10.7}$  index near 70. During periods of the weak magnetic activity in summer, Poker Flat may behave as a midlatitude station much of the time. In this paper we define weak magnetic activity as those periods, free of

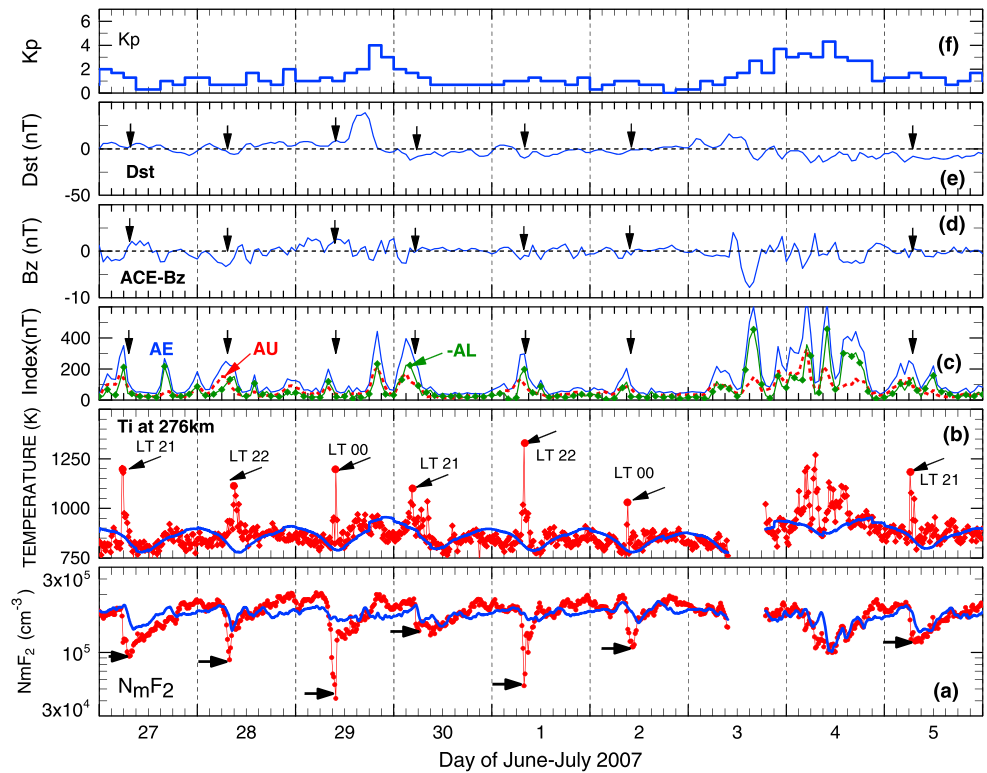


**Figure 1.** (a) Measured and modeled  $N_mF_2$ , (b) ion temperature, (c) magnetic activity indices  $AE$  (solid line),  $-AL$  (diamonds), and  $AU$  (dashed line), (d) Earth-shifted  $B_z$  from ACE, (e)  $Dst$ , and (f)  $K_p$  for 27 June to 5 July 2007. The red lines with symbols in Figures 1a and 1b represent the PFSIR data and the blue lines without symbols represent the FLIP model calculations not including ion convection. The arrows identify the occurrence times of the  $T_i$  spikes and density depletions with approximate solar apparent time shown in Figures 1b. The vertical grid lines are for 00 UT (~13.0 MLT, ~14.2 LT).

magnetic storms, where  $K_p \leq 3$  and the change in the  $Dst$  was less than 25 nT in magnitude for 12 h or more prior to the event.

#### 4.1. Comparisons for 27 June to 5 July 2007

Figure 1 shows an example of density depletions and ion temperature spikes in the PFSIR data at 276 km altitude for 27 June to 5 July 2007. The local times (LT) of the premidnight  $T_i$  spikes and density depletions are shown on Figure 1b. The local time referred to in this paper is solar apparent time, which is important for determining solar zenith angle (SZA). Magnetic local time (MLT) is approximately 1 h less than local solar time at Poker Flat.

Figure 1 also shows key magnetic activity indices for the period:  $K_p$ ,  $Dst$ ,  $AU$ ,  $-AL$ , and  $AE$ . The  $K_p$  and  $Dst$  indices show a weak level of magnetic activity, except for late on 29 June and also on 4 July. The ACE satellite Earth-shifted  $B_z$  shows small southward excursions before or during the density depletions. However, there is not a one-to-one correspondence between negative  $B_z$  excursions and the occurrence of  $T_i$  spikes and density depletions. The  $AE$  index shows strong excursions near the time of the density troughs that typically have a half-life of one to three hours.

The  $T_i$  variability can be a good indicator of enhanced magnetic activity as can be seen by the rapid variation in  $T_i$  on 4 July. The deep density depletions are not usually seen during periods of enhanced magnetic activity, most likely because the plasma arriving at Poker Flat is transported antisunward across the sunlit polar region. In fact, weak magnetic activity is necessary for the identification of the density depletions and the corresponding isolated ion temperature spikes at Poker Flat. The density depletions and isolated ion temperature spikes are seen on most nights during 27 June to 5 July 2007 but are more episodic at other summer periods between May 2007 and August 2008. The isolated  $T_i$  spikes in this paper typically last less

than 1 h, while the density depletions last from 1 to 3 h. The solar zenith angle did not exceed  $93^\circ$  during this period. This is important because the peak density should decay only moderately under these conditions.

The density depletion on 27 June occurs near 21 LT when the SZA is  $90^\circ$ . In this case  $B_z$  was negative for  $\sim 5$  h prior to the ionospheric response. The model shows only a small diurnal variation partly because the nighttime neutral winds drive the plasma to higher altitudes where the decay is slowed.

The blue solid lines without symbols in Figure 1 are from the standard FLIP model that does not include ion convection. The arrows in Figure 1b indicate the height and time of the Ti spikes while the arrows in the other panels just identify the times when the spikes occur. Below 300 km, the standard FLIP model ion temperature is only slightly above the NRLMSISE-00 model neutral temperature and there is generally satisfactory agreement between the modeled and measured Ti data, except for the premidnight spikes.

Comparison of Figures 1a and 1b shows that the Ti spikes usually occur around the same time as large depletions in  $N_m F_2$ . The density recovers to normal nighttime values near midnight when the SZA is at its maximum. The sudden decrease of the electron density is particularly striking and not typical of normal nighttime decay. It suggests that the radar has encountered an electron density trough. There is a tendency for the model electron density to decrease in the evening on several days but it does not reproduce the very steep density depletions that are observed. It is difficult to explain the sudden decreases in electron density when the high-latitude ionosphere remains sunlit for most of the day and the normal two-cell convection pattern should bring relatively dense plasma from regions that are still sunlit.

Except around the time of the sudden density depletions, the model  $N_m F_2$  agrees well with the PFISR measurement between 00 UT and 14 UT on most days. On the other hand, the model underestimates the measured  $N_m F_2$  during the periods of smallest SZA between 18 UT and 23 UT. The solar EUV irradiances are unlikely to be the cause of this underestimation because the FLIP model  $N_m F_2$  generally agrees well with the PFISR data throughout the winter and equinoxes in 2007 and the solar activity did not vary much in 2007. Based on neutral densities inferred from the TIMED-GUVI instrument, *Richards et al.* [2009] suggested that the underestimate of the density in the summer of 2007 may indicate a problem with the NRLMSISE-00 model O to  $N_2$  density ratio in the middle of the day in this geographical region during this period of unusually weak solar and magnetic activity.

Figure 2 shows the  $N_m F_2$ ,  $h_m F_2$ , and inferred poleward winds for the same 27 June to 5 July period as in Figure 1 along with ion convection velocities for 28 June. The radar convection velocities are not available for the other days during this period. The ion velocities were determined  $\sim 2^\circ$  north of PFISR. The observed ion convection velocities do not vary greatly between  $66$  and  $68^\circ$  magnetic. The crosses in Figure 2a show the model  $N_m F_2$  that is calculated when ion convection is taken into account as explained in the next section. The large westward ion convection velocities measured by the radar for 28 June in Figure 2b provide experimental confirmation that ion convection is involved in producing the density depletions and Ti spikes. The convection velocities are in the magnetic frame of reference, which corotates with the Earth and is tilted toward the American sector by approximately  $11^\circ$ . At Poker Flat the magnetic declination is  $\sim 22^\circ$ . Although the velocities were measured  $\sim 2^\circ$  north of PFISR, they are likely to be similar overhead at Poker Flat because the convection velocities are consistent with the magnitudes of the observed increases in Ti. The frictional heating from the observed convection velocity of 800 m/s could produce the observed Ti enhancement of 200–250 K on 28 June depending on the strength and direction of the neutral wind [*Goodwin et al.*, 2014].

Figure 2c shows that there is generally good agreement between the equivalent neutral winds inferred from  $h_m F_2$  and the radar magnetic meridional neutral winds inferred from the field-aligned ion velocity. The winds follow a typical midlatitude pattern being small and poleward during the day and larger and equatorward during the night. Neither of the inferred neutral winds is likely to be accurate during the Ti spike events because the expansion during heating could cause the ions to move upwards with possibly high velocities. From the point of view of electron density modeling, reproducing  $h_m F_2$  is more important than the relative combination of wind and meridional electric field drift. It must be borne in mind that these winds are in the magnetic meridian and frictional heating from westward ion convection would be negligible. However, the neutral winds probably have a large magnetically eastward component because winds tend to blow equatorward in geographic coordinates. This together with the onset of convection helps explain why the Ti spikes preferentially occur in the premidnight sector as proposed by *Goodwin et al.* [2014].

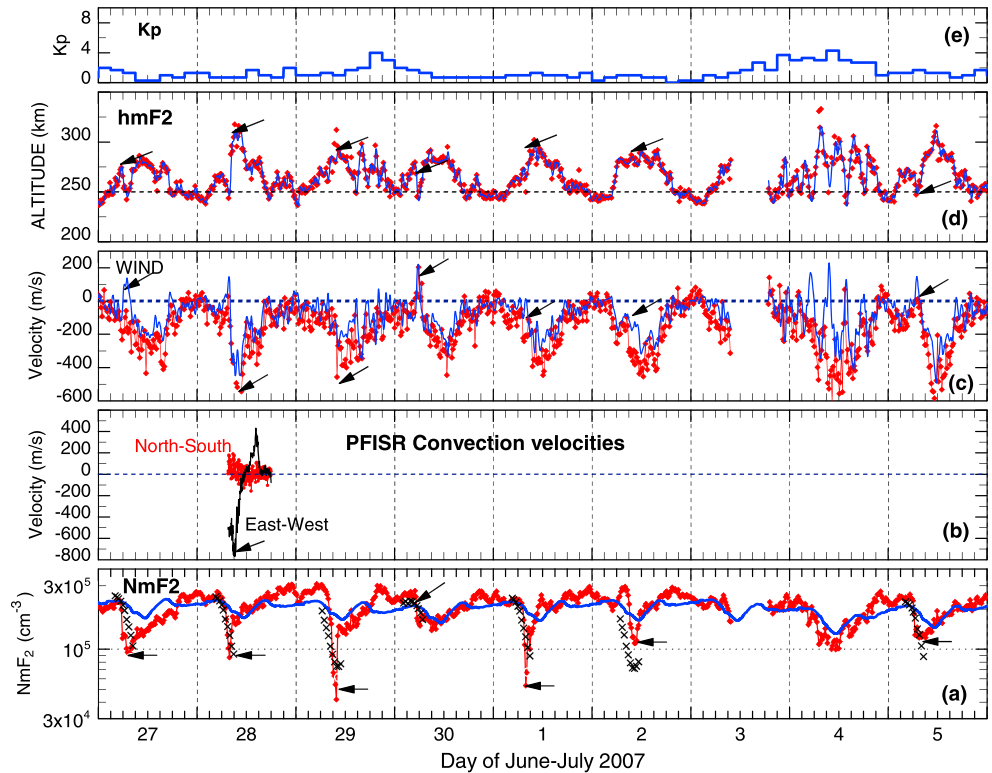


**Figure 2.** (a) Measured and modeled  $N_mF_2$ , (b) measured eastward and northward convection velocities, (c) poleward winds inferred from the ISR and  $h_mF_2$ , (d) measured and modeled  $h_mF_2$  for 27 June to 5 July 2007. The red lines with symbols are the measured values. The solid blue line without symbols in Figure 2a is the modeled  $N_mF_2$  for Poker Flat using the LT average neutral wind without convection electric fields. The crosses show the model  $N_mF_2$  when ion convection from (55°N, 240°E) is included. The arrows identify the occurrence times of the spikes. (e) The  $K_p$  magnetic activity index.

Figure 2d shows that there is not a consistent signature in  $h_mF_2$  at the time of the Ti spikes and density depletions. The solid blue line shows that the model closely follows the measured  $h_mF_2$  while ignoring outlier points where the change in height is unphysical.

#### 4.2. Simulations With Convection Included for 27 June to 5 July 2007

The  $O^+$  reaction rates are strongly temperature dependent for temperatures above about 1500° K [St.-Maurice and Torr, 1978], and it has been shown that enhanced ion convection can create low electron densities due to increased effective temperatures [Banks et al., 1974; Schunk et al., 1975, 1976]. This explanation is unlikely for the 2007 and 2008 observations because the observed convection velocities and ion temperatures are not large enough to greatly affect the reaction rates. It has also been suggested that the steep depletion in electron density may result from an increase in the  $O^+$  loss rate because the  $O^+ + N_2$  loss rate is a strong function of vibrational excitation of  $N_2$ . However, the FLIP model includes vibrational excitation of  $N_2$  and the effect on the  $O^+$  loss rate is small for these solar minimum conditions.

Poker Flat is also a special place in the Northern Hemisphere because the offset of the magnetic field in the night sector pushes the auroral activity to lower geographic latitudes. In addition, the oval region is offset antisunward from the magnetic pole. As a result, PFISR comes into the convection region and out of it roughly around dawn and dusk. For active conditions the oval has expanded and the radar spends more time inside the oval. For very quiet conditions it never sees the auroral oval.

To determine if the observed density depletions could be created without increasing the  $O^+$  reaction rates, the model was run with several ion convection paths to Poker Flat. Because the actual convection path and velocity along that path are unknown it is necessary to make some assumptions. Figure 3 shows an example convection pattern from the Super Dual Auroral Radar Network (SuperDARN) near the time of the density

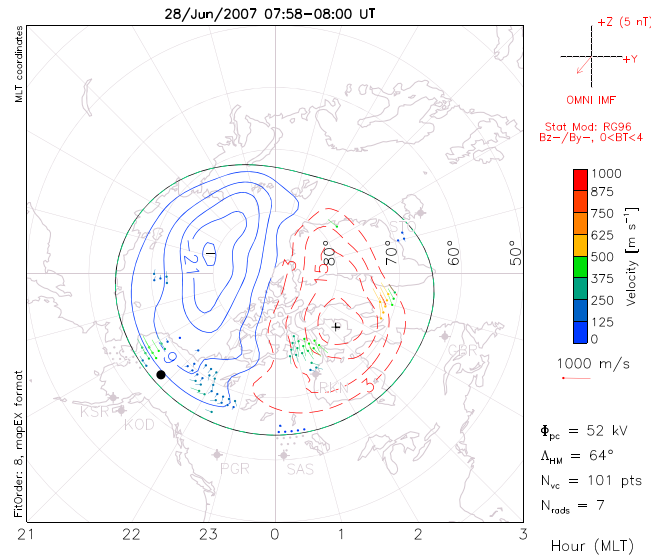


**Figure 3.** SuperDARN convection pattern near the time of the density trough on 28 June 2007 (<http://vt.superdarn.org/tiki-index.php?page=DaViT+Map+Potential+Plot>). Poker Flat is the dot located near the equatorward edge of the convection pattern at 65° magnetic and approximately 21 MLT.

This suggests that the trough plasma arriving at Poker Flat has its origin instead farther to the south and east of Poker Flat where the solar zenith angle is larger.

As noted above, the actual convection speeds and paths to Poker Flat are unknown. All that is known is the strongest convection is typically westward with a speed of ~800 m/s as observed in the vicinity of Poker Flat. The model calculations indicate that the amount of time spent in darkness is more important than the actual convection path. Figure 4 shows some possible convection paths arriving at Poker Flat with the observed characteristics. A direct path from point A would follow a line of constant magnetic declination (~22°) and take about 1 h. However, if there were a northward drift, it could follow a path from point A like that shown in Figure 4. A path from point B could follow the magnetic parallel to Poker Flat and take about 2 h. For cases A and B, plasma would have been corotating eastward until it meets an electric field that produces a strong magnetically westward convection in the premidnight sector. The electric field could be enabled by the low postsunset densities at the lower latitudes, which inhibit current closure (see Anderson et al. [1991, 2001] for details). This mechanism has similarities with that for a Sub-Auroral Ion Drift (SAID) as envisaged by Spiro et al. [1978].

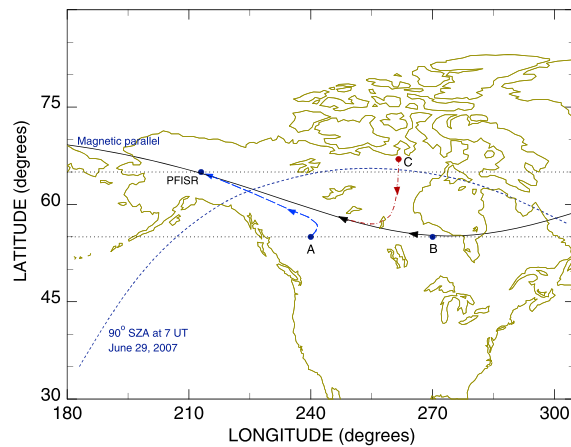


**Figure 4.** Some possible ion convection paths to Poker Flat. The magnetic parallel is in corrected geomagnetic coordinates. A path from point A has a length of approximately 3000 km and it takes approximately 1 h to reach Poker Flat with a speed of 800 m/s. Paths from points C and D take approximately 2 h to reach Poker Flat with a speed of 800 m/s. The short dashed line shows the terminator (SZA = 90°) at 7 UT on 29 June 2007.

trough on 28 June 2007. SuperDARN convection patterns are available for all the days studied and Figure 3 is representative of the situation when the troughs occur. Poker Flat is located near the equatorward edge of the convection pattern at 65° magnetic and approximately 21 MLT. Figure 2 of Goodwin et al. [2014] shows a similar SuperDARN pattern for 27 June. Examination of other SuperDARN convection patterns in 2007 and 2008 reveals that the deepest density troughs tend to occur in the dusk-midnight sector, according to the SuperDARN convection pattern. Convection along closed loops like the outermost contour in Figure 3 on the duskside cannot cause a significant density trough at Poker Flat in summer because the solar zenith angle is always less than 93° along this path.

Convection along path C is the type of path that results from a two-cell convection pattern with flow across the polar cap and would also take ~2 h to reach Poker Flat from point C at 800 m/s. This is the path that plasma would take to Poker Flat when the edge of the convection pattern expands beyond 65° magnetic latitude the convection paths bring plasma from recently sunlit regions, which would cause

only moderate density depletions. In fact, the SuperDARN convection patterns indicate that is most likely the case on 4 July.

In 2007, the corrected geomagnetic latitude at Poker Flat was  $\sim 65^\circ\text{N}$  and the magnetic declination was  $\sim 22^\circ$  east at 300 km altitude above Poker Flat. Following a line of constant magnetic declination, convection with a velocity of  $\sim 800$  m/s could bring plasma to Poker Flat from the vicinity of  $55^\circ$  north latitude and  $240^\circ$  east longitude (see Figure 4). At this geographic location, sunset occurs earlier in the evening relative to Poker Flat because of the lower geographic latitude and also because of the difference in longitude. In all, the electron density at ( $55^\circ\text{N}$ ,  $240^\circ\text{E}$ ) has had 3 to 4 h to decay after sunset before being swept to Poker Flat. The plasma at point B has an additional 2 h of decay time and this could result in lower densities than at point A.

The crosses in Figure 2a show the model densities at half hour intervals when the plasma comes from ( $55^\circ\text{N}$ ,  $240^\circ\text{E}$ ) and arrives at Poker Flat 1 h later. The  $N_mF_2$  comparison in Figure 2a shows that this convection pattern can produce sudden deep density depletions without the need for increased reaction rates or prolonged flow stagnation. The solid blue line in Figure 2a is for the location of PFISR using the local time variation of the median equivalent neutral wind shown in Figure 2c without taking into account ion convection. This calculation serves as a reference for the extent of the decrease in model density from the effect of convection represented by the crosses.

There is especially good model-data agreement on 28 June when the measured convection velocities are available. All of the crosses in Figure 2a were produced with the same convection velocity and direction. Even so, this simple convection pattern produces different densities depending on arrival time at Poker Flat. There is little or no reduction in model density at Poker Flat prior to  $\sim 05$  UT when it would bring high-density plasma from a recently sunlit source region where the density has not had sufficient time to decay. In addition, the solar zenith angle is still less than  $90^\circ$  at Poker Flat at that time. There are no crosses following the density minimum because the measured ion PFISR convection patterns typically show a sharp transition from westward to eastward flow on the midnight side of the depletions.

Clearly, there are significant uncertainties related to the convection assumptions. For example, the velocity and duration of the westward convection may vary along the path or there may be convection in the magnetic meridian. For this reason, model calculations were carried out for several convection paths at different longitudes between points A and B as well as for path C. All the convection paths from points A to B produce similar densities at Poker Flat, but the densities from path C are a factor of 2 or more higher because the plasma has much less time at large solar zenith angles. Given the path uncertainties, all the convection calculations presented in this paper used path A to represent all the possible convection trajectories from lower latitudes.

Another uncertainty concerns the variation of the neutral wind that the plasma experiences before it reaches Poker Flat. There is no empirical wind model with reliability that is comparable to the NRLMSISE-00 neutral density model. So, the convection simulations used the median local time variation of the Poker Flat equivalent winds from the 27 June to 5 July to ensure that  $h_mF_2$  is well modeled when the plasma arrives at Poker Flat. The solid blue line in Figure 2a shows the model peak electron density at Poker Flat from the model run using the median LT wind variation when there is no model convection. This simulation is to show that the median winds produce  $h_mF_2$  and  $N_mF_2$  values that are very close to those obtained in Figure 1a when the model used the wind derived from the actual PFISR  $h_mF_2$  data. The assumption that the local time wind variation is similar at different longitudes is reasonable but there will be some wind uncertainty because of possible latitudinal wind variation. If the equatorward winds were smaller below  $65^\circ$  latitude, the model densities would also be smaller.

### 4.3. Comparisons for 13–22 July 2008

The  $F_{10.7}$  solar activity index was even lower in 2008 than in June 2007 with the 81 day average near 66 in the summer of 2008. Figure 5 shows an example of density depletions and ion temperature spikes in the PFISR data at 276 km altitude for 13–22 July 2008.

The solar apparent times of the premidnight density depletions are shown in Figure 5b. Figure 5 also shows key magnetic activity indices for the period. The  $K_p$  and  $Dst$  indices show a very low level of magnetic activity on 19 and 20 July and there are no Ti spikes or density depletions and the model reproduces  $N_mF_2$  very well on these days. The ACE satellite Earth-shifted  $B_z$  shows small southward incursions several hours before

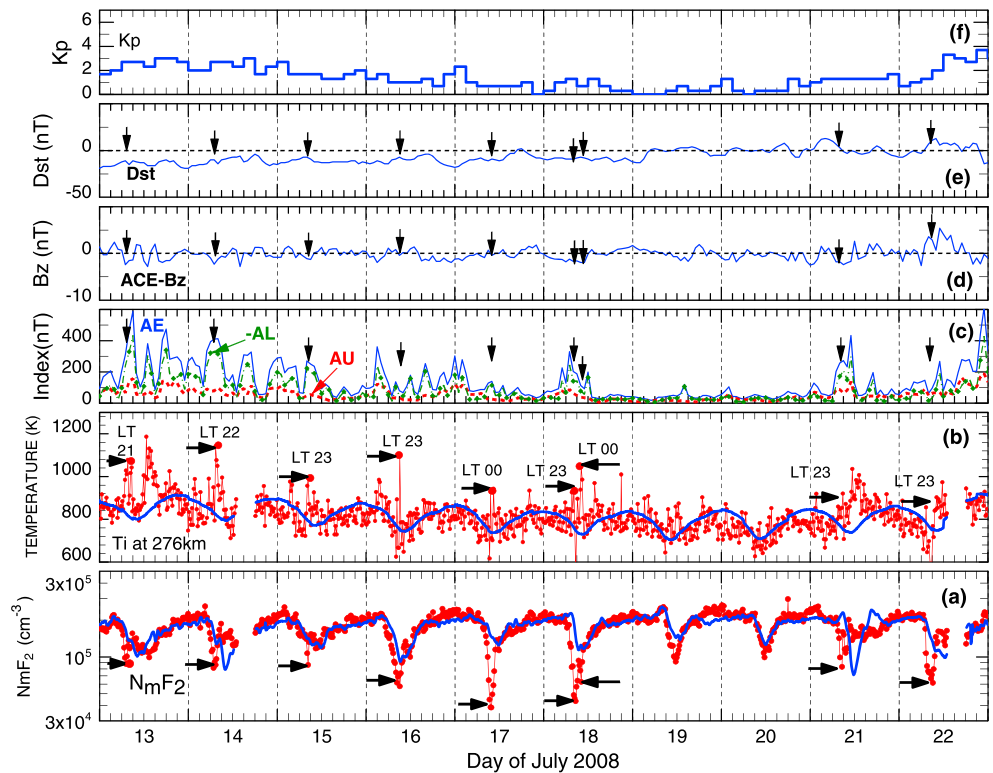


**Figure 5.** Measured and modeled (a)  $N_mF_2$ ; (b) ion temperature; (c) magnetic activity indices  $AE$ ,  $-AL$ , and  $AU$ ; (d) Earth-shifted  $B_z$  from ACE; (e)  $Dst$ ; (f) and  $K_p$  for 13–22 July 2008. The red lines with symbols in Figures 5a and 5b represent the PFISR data and the blue lines without symbols represent the FLIP model calculations not including ion convection. The arrows identify the occurrence times of the  $T_i$  spikes and density depletions with approximate solar local time shown in Figure 5b. The vertical grid lines are for 00 UT ( $\sim 13$  MLT,  $\sim 14.2$  LT).

several of the density depletions, with the notable exception of the large depletion on 17 July, which is also devoid of activity in the  $AE$  index. The  $AE$  index shows strong fluctuations on 13–15 July, which may indicate the existence of regular substorms. The  $T_i$  spikes are not as clearly defined as in 2007 and there are sometimes density troughs without clearly defined  $T_i$  spikes in the summer of 2008. Therefore, the arrows identify the time of the deep density depletions rather than  $T_i$  spikes.

The blue solid line without symbols in Figure 5a shows that the peak density from the standard FLIP model agrees exceptionally well with the data most of the time during this period when using the measured  $h_mF_2$  and the SEE EUV irradiances. The densities on these very quiet days provide a useful reference to gauge the extent of the density depletions on the other days. The better model-data agreement in summer 2008 as compared to 2007 results from the measured densities being lower in 2008, even though the solar and magnetic activities were similar.

Figure 6 shows the peak electron density (a), northward and eastward convection velocities (b), model equivalent wind (c),  $h_mF_2$  (d), and  $K_p$  magnetic activity index (e). The solid blue line in Figure 6a is for the location of PFISR using the local time variation of the median equivalent neutral wind shown in Figure 6c without taking into account ion convection. This calculation serves as a reference for the extent of the decrease in model density from the effect of convection represented by the crosses. The SuperDARN convection patterns at the times of the deep density troughs during this July 2008 period are similar to the pattern in Figure 3, in that the convection barely reaches Poker Flat.

Note that the PFISR convection velocities can be strong for several hours in the premidnight sector before the density depletions, which mainly occur closest to midnight where there are the largest spikes in the westward convection velocities, followed soon after by eastward convection. The strongest westward convection typically lasts for 1 to 2 h. It is likely that the earliest convection velocities are part of the normal

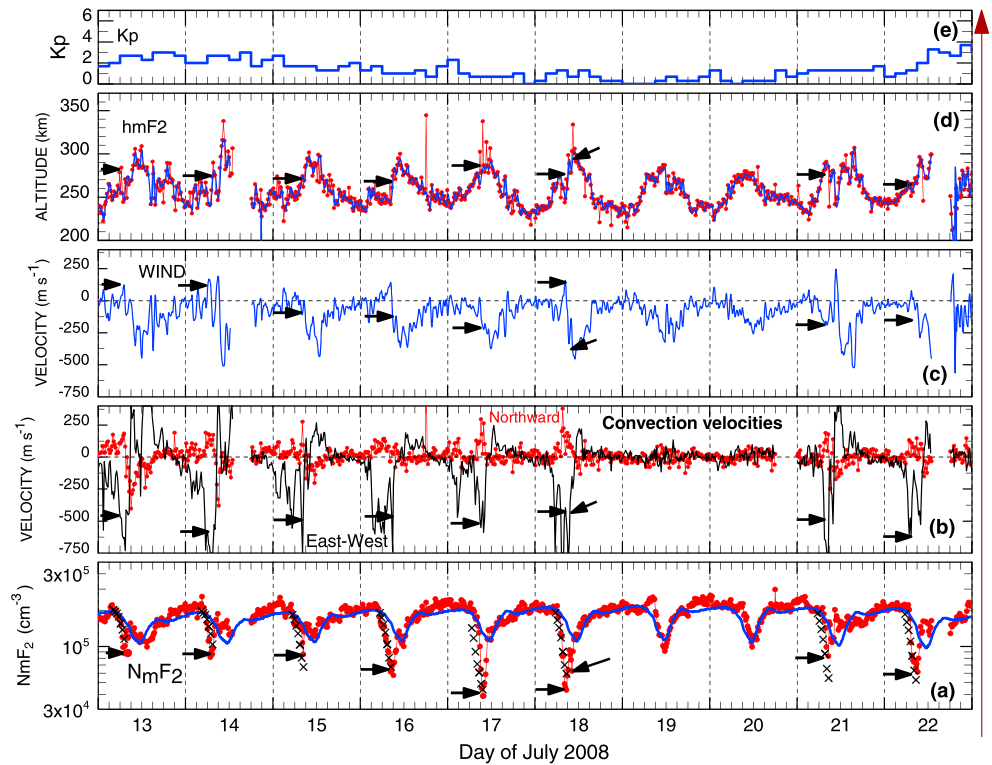


**Figure 6.** (a) Comparison of PFISR data with the FLIP model  $N_mF_2$  at Poker Flat with convection (crosses) and without convection (solid blue line), (b) measured convection velocities, (c) poleward winds inferred from  $h_mF_2$ , (d) modeled and measured  $h_mF_2$  for 13–22 July 2008. The red lines with symbols are the measured values. The solid blue line without symbol in Figure 6a is the modeled  $N_mF_2$  with the median wind and no convection electric fields. The crosses show the model  $N_mF_2$  including ion convection from (55°N, 240°E). The arrows identify the occurrence times of the density depletions near 21 LT. (e) The Kp magnetic activity index.

two-cell convection pattern that may not even reach as far south as Poker Flat. The northward convection velocities are small most of the time. However, there are enhanced northward convection velocities ( $> 250$  m/s) at the times of the density depletions on 17 and 18 July. Northward convection is important because it can help bring low-density plasma from lower latitudes.

The crosses in Figure 6a show the results of model runs with convection paths that start from (55°N, 240°E) and arrive at Poker Flat 1 h later at half hour intervals. There is an unusually gradual density decay on 16 July when the decrease begins unusually early at ~0500 UT, which the model crosses capture very well. On the other hand, although the minimum density is well captured on 17 July, the model decrease starts too early. In general, model-data differences can most likely be attributed to the actual convection being more complicated than the simple assumed convection. The presence of a deep trough on 17 July is also unusual because the magnetic activity was weak and similar to that on 19 and 20 July when there were no troughs. Overall, the model shows that simple convection paths can capture the deep density depletions that are observed at Poker Flat.

#### 4.4. Epoch Study

Figure 7 shows epoch studies for 20 trough events identified in 2007 and 23 in 2008. Zero time is centered on the time of premidnight minimum in the measured  $N_mF_2$  for each event. The median UT for the  $N_mF_2$  minimum was 8.7 in 2007 and it was 8.4 in 2008. These times are approximately 23 LT (22 MLT). The earliest time of occurrence was approximately 7 UT in both years and the latest time of occurrence was ~11 UT in 2007 and 10 UT in 2008. The solid blue lines show the PFISR median data for the trough events while the broken red lines show the PFISR medians for the whole of the summer (May, June, and July) data (including the solid blue line events) for each year, centered on 23 LT.

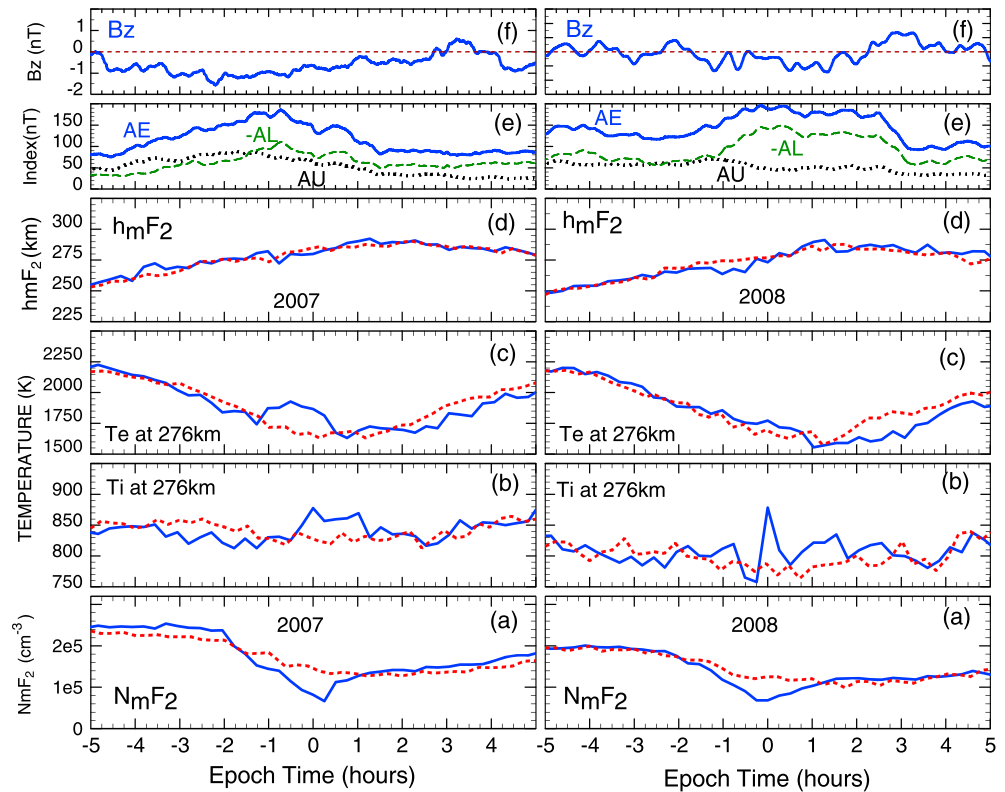


**Figure 7.** Epoch study on  $N_mF_2$ , Ti, Te,  $h_mF_2$ , AE, AU,  $-AL$ , and Bz, centered on the time of the electron density minimum in (left) 2007 and (right) 2008. The solid lines are medians for 20 events in 2007 and 23 events in 2008. The zero epoch time is approximately 8.5 UT (23 LT, 22 MLT) in both years. The dashed red lines are medians for all the PFISR measurements for May–July in each year centered on 23 LT.

In both 2007 and 2008, the median  $N_mF_2$  drops from  $\sim 2 \times 10^5$  to  $\sim 7 \times 10^4 \text{ cm}^{-3}$  in 2 h for the trough cases. The ion temperature (Ti) shows a broad peak between 0 and 1 h epoch time (ET) in 2007 and stronger peak at 0 ET in 2008. It is of interest that Ti is generally about 50°K higher in 2007 than in 2008. Since Ti and Tn are closely coupled at 276 km, this most likely indicates that the thermosphere was cooler in 2008. The median of all the summer data also indicates that there is a nighttime Ti minimum in 2008 but not in 2007.

There is a small peak in the median Te in 2007 that mirrors the trough in  $N_mF_2$ . This is what would be expected theoretically whenever the electron density decreases in the presence of local heating or a topside ionosphere heat flux. On the other hand, there is no Te peak in 2008 even though the change in  $N_mF_2$  is similar. There is little difference in  $h_mF_2$  between 2007 and 2008 and the behavior at 0 ET is not unusual in either year. The AE index has a definite maximum encompassing 0 ET in both years. However, there is not a definitive signal in the median magnetic field Bz component, which is mildly negative for several hours prior to the density minimum in 2007, but not in 2008.

The deep density troughs appear to occur when enhanced magnetic activity brings the edge of the two-cell convection pattern to the Poker Flat latitude. It is proposed that, under these circumstances, plasma, which has been corotating in darkness at lower latitudes, can be quickly convected to Poker Flat. It is possible that this process is ubiquitous near the edge of the dusk convection cell when the convection zone is expanding but is only observed at Poker Flat under the right circumstances. If the convection pattern expands too far beyond Poker Flat, no deep troughs are observed by PFISR because the convection paths bring relatively dense, recently sunlit plasma to Poker Flat. On the other hand, under very quiet conditions when the dusk convection does not reach as far south as Poker Flat as on 19 and 20 July 2008 the density behavior resembles that of the midlatitude ionosphere.

## 5. Discussion and Conclusions

This study is focused on premidnight electron density behavior during a period of weak solar and magnetic activity in the summer of 2007 and 2008. Summer is a special case because it is difficult to produce sudden electron density depletions at Poker Flat when the Sun barely sets in the high-latitude ionosphere. The equinox and winter seasons are not considered for this study because premidnight sudden density depletions cannot easily be isolated from the natural steep decay that occurs after sunset. Magnetically disturbed times are excluded because isolated premidnight density depletions are not identifiable due to strong and variable convection and particle precipitation that can produce highly variable densities and temperatures.

The sudden and deep density depletions associated with strong convection reported in this paper resemble the SAID phenomena. A SAID is a very narrow convection channel ( $\sim 1^\circ$  latitude) that is imbedded in a broader convection channel ( $\sim 5^\circ$  latitude) known as a subauroral polarization stream (SAPS) that was been defined by Foster and Burke [2002]. The essential properties of SAIDs have been summarized by Wang and Luhr [2011]. Erickson *et al.* [2011] examined Millstone Hill incoherent scatter radar data collected over two solar cycles between 1979 and 2001 to determine average SAPS characteristics. For low magnetic activity, the latitudes and times of SAPS occurrence in the Millstone Hill data agree well with the occurrence times in the PFISR trough events [see Erickson *et al.*, 2011, Figure 2].

In summary, it is envisaged that PFISR encounters a SAPS-like density trough in the evening as a result of convection to Poker Flat of low-density plasma that has been corotating in darkness for several hours south and east of Poker Flat. The radar then rotates across the trough into a region near midnight where the plasma has been decaying normally and the density is still relatively high.

### Acknowledgments

This research was supported by NASA grant NNX09J76G and NSF grant AGS-1048350 to George Mason University. J.S.M. was funded by the Canada Research Chair program. L.G. was funded by the Canadian NSERC. The Poker Flat Incoherent Scatter Radar is operated by SRI International on behalf of the U.S. National Science Foundation under NSF Cooperative Agreement AGS-1133009. Work at SRI was supported by NSF grants AGS-1133009 and AGS-1242913. We acknowledge use of NASA/GSFC's Space Physics Data Facility's OMNIWeb (or CDAWeb or ftp) service, and OMNI magnetic field data. J.M.R. acknowledges the support of NSF grant AGS-1243070. The authors acknowledge the use of SuperDARN data. SuperDARN is a collection of radars funded by national scientific funding agencies of Australia, Canada, China, France, Japan, South Africa, United Kingdom, and United States of America.

Alan Rodger thanks Pam Calliham and another reviewer for their assistance in evaluating this paper.

### References

- Anderson, P. C., R. A. Heelis, and W. B. Hanson (1991), The ionospheric signatures of rapid subauroral ion drifts, *J. Geophys. Res.*, *96*, 5785–5792, doi:10.1029/90JA02651.
- Anderson, P. C., D. L. Carpenter, K. Tsuruda, T. Mukai, and F. J. Rich (2001), Multisatellite observations of rapid subauroral ion drifts (SAID), *J. Geophys. Res.*, *106*, 29,585–29,599, doi:10.1029/2001JA000128.
- Aponte, N., M. J. Nicolls, S. A. Gonzalez, M. P. Sulzer, M. C. Kelley, E. Robles, and C. A. Tepley (2005), Instantaneous electric field measurements and derived neutral winds at Arecibo, *Geophys. Res. Lett.*, *32*, L12107, doi:10.1029/2005GL022609.
- Banks, P. M., R. W. Schunk, and W. J. Raitt (1974),  $\text{NO}^+$  and  $\text{O}^+$  in the high latitude F-region, *Geophys. Res. Lett.*, *1*, 239–242, doi:10.1029/GL001i006p00239.
- Buonsanto, M. J., and O. G. Witasse (1999), An updated climatology of thermospheric neutral winds and F region ion drifts above Millstone Hill, *J. Geophys. Res.*, *104*, 24,675–24,687, doi:10.1029/1999JA900345.
- Dyson, P. L., T. P. Davies, M. L. Parkinson, A. J. Reeves, P. G. Richards, and C. E. Fairchild (1997), Thermospheric neutral winds at southern mid-latitudes: A comparison of optical and ionosonde  $h_m F_2$  methods, *J. Geophys. Res.*, *102*, 27,189–27,196, doi:10.1029/97JA02138.
- Erickson, P. J., F. Beroz, and M. Z. Miskin (2011), Statistical characterization of the American sector subauroral polarization stream using incoherent scatter radar, *J. Geophys. Res.*, *116*, A00J21, doi:10.1029/2010JA015738.
- Foster, J. C., and W. J. Burke (2002), SAPS: A new characterization for sub-auroral electric fields, *Eos Trans. AGU*, *83*, 393, doi:10.1029/2002EO000289.
- Goodwin, L., J.-P. St.-Maurice, P. Richards, M. Nicolls, and M. Hairston (2014), F region dusk ion temperature spikes at the equatorward edge of the high-latitude convection pattern, *Geophys. Res. Lett.*, *41*, 300–307, doi:10.1002/2013GL058442.
- Heinselman, C. J., and M. J. Nicolls (2008), A Bayesian approach to electric field and E-region neutral wind estimation with the Poker Flat Advanced Modular Incoherent Scatter Radar, *Radio Sci.*, *43*, RS5013, doi:10.1029/2007RS003805.
- Nagy, A. F., and P. M. Banks (1970), Photoelectron fluxes in the ionosphere, *J. Geophys. Res.*, *75*, 6260–6270, doi:10.1029/JA075i031p06260.
- Picone, J. M., A. E. Hedin, D. P. Drob, and A. C. Aikin (2002), NRLMSISE-00 empirical model of the atmosphere: Statistical comparisons and scientific issues, *J. Geophys. Res.*, *107*(A12), 1468, doi:10.1029/2002JA009430.
- Richards, P. G. (1991), An improved algorithm for determining neutral winds from the height of the F2 peak electron density, *J. Geophys. Res.*, *96*, 17,839–17,846, doi:10.1029/91JA01467.
- Richards, P. G. (2001), Seasonal and solar cycle variations of the ionospheric peak electron density: Comparison of measurement and models, *J. Geophys. Res.*, *106*, 12,803–12,819, doi:10.1029/2000JA000365.
- Richards, P. G. (2002), Ion and neutral density variations during ionospheric storms in September 1974: Comparison of measurement and models, *J. Geophys. Res.*, *107*(A11), 1361, doi:10.1029/2002JA009278.
- Richards, P. G. (2004), On the increases in nitric oxide density at mid latitudes during ionospheric storms, *J. Geophys. Res.*, *109*, A06304, doi:10.1029/2003JA010110.
- Richards, P. G., P. L. Dyson, T. P. Davies, M. L. Parkinson, and A. J. Reeves (1998), The behavior of the ionosphere and thermosphere at a southern mid-latitude station during magnetic storms in early March 1995, *J. Geophys. Res.*, *103*, 26,421–26,432, doi:10.1029/97JA03342.
- Richards, P. G., et al. (2000), On the relative importance of convection and temperature on the behavior of the ionosphere in North America during January, 6–12, 1997, *J. Geophys. Res.*, *105*, 12,763–12,776, doi:10.1029/1999JA000253.
- Richards, P. G., M. J. Nicolls, C. J. Heinselman, J. J. Sojka, J. M. Holt, and R. R. Meier (2009), Measured and modeled ionospheric densities, temperatures, and winds during the IPY, *J. Geophys. Res.*, *114*, A12317, doi:10.1029/2009JA014625.
- Richards, P. G., R. R. Meier, and P. J. Wilkinson (2010), On the compatibility of satellite measurements of thermospheric composition and solar EUV irradiance with ground-based ionospheric electron density data, *J. Geophys. Res.*, *115*, A10309, doi:10.1029/2010JA015368.

- Salah, J. E., and J. M. Holt (1974), Midlatitude thermospheric winds from incoherent scatter radar and theory, *Radio Sci.*, *9*, 301–313, doi:10.1029/RS009i002p00301.
- Schunk, R. W., W. Raitt, and P. Banks (1975), Effect of electric fields on the daytime high latitude *E* and *F* regions, *J. Geophys. Res.*, *80*, 3121–3130, doi:10.1029/JA080i022p03121.
- Schunk, R. W., P. Banks, and W. Raitt (1976), Effects of electric fields and other processes upon the nighttime high latitude *F* layer, *J. Geophys. Res.*, *81*, 3271–3282, doi:10.1029/JA081i019p03271.
- Sojka, J. J., M. J. Nicolls, C. J. Heinselman, and J. D. Kelly (2009), The PFISR IPY observations of ionospheric climate and weather, *J. Atmos. Sol. Terr. Phys.*, *71*, 771, doi:10.1016/j.jastp.2009.01.001.
- Spiro, R. W., R. A. Heelis, and W. B. Hanson (1978), Ion convection and the formation of the mid-latitude *F* region ionization trough, *J. Geophys. Res.*, *83*, 4255–4264, doi:10.1029/JA083iA09p04255.
- St.-Maurice, J.-P., and D. G. Torr (1978), Nonthermal rate coefficients in the ionosphere: The reaction of  $O^+$  with  $N_2$ ,  $O_2$ , and  $NO$ , *J. Geophys. Res.*, *83*, 969–977, doi:10.1029/JA083iA03p00969.
- Torr, M. R., D. G. Torr, P. G. Richards, and S. P. Yung (1990), Mid- and low-latitude model of thermospheric emissions: 1.  $O^+(^2P)$  7320 Å and  $N_2(^2P)$  3371 Å, *J. Geophys. Res.*, *95*, 21,147–21,168, doi:10.1029/JA095iA12p21147.
- Wang, H., and H. Luhr (2011), The efficiency of mechanisms driving Subauroral Polarization Streams (SAPS), *Ann. Geophys.*, *29*, 1277–1286, doi:10.5194/angeo-29-1277-2011.
- Woods, T. N., et al. (2008), XUV photometer system (XPS): Improved solar irradiance algorithm using Chianti spectral models, *Sol. Phys.*, doi:10.1007/s11207-008-9196-6.